# Cyclosporin A but not FK506 activates the integrated stress response in human cells

Anthony Fedele, Valérie Carraro, Jianling Xie, Julien Averous, Christopher Proud

JBC ARTICLE

# Cyclosporin A but not FK506 activates the integrated stress response in human cells

Received for publication, May 24, 2020, and in revised form, July 28, 2020 Published, Papers in Press, August 24, 2020, DOI 10.1074/jbc.RA120.014531

**Anthony O. Fedele[1], Valérie Carraro[2], Jianling Xie (建凌 谢)[3], Julien Averous[2], and Christopher G. Proud[1,3,4,*]**

[1]*Hopwood Centre for Neurobiology, Lifelong Health Theme, South Australian Health & Medical Research Institute, North Terrace Campus, Adelaide, Australia,* [2]*INRAE, Unité de Nutrition Humaine, Université Clermont Auvergne, Clermont-Ferrand, France,* [3]*Lifelong Health Theme, South Australian Health & Medical Research Institute, North Terrace Campus, Adelaide, Australia, and* [4]*School of Biological Sciences, University of Adelaide, North Terrace Campus, Adelaide, Australia*

Edited by Roger J. Colbran

**Cyclosporin A (CsA) and tacrolimus (FK506) are valuable immunosuppressants for a range of clinical settings, including (but not limited to) organ transplantation and the treatment of autoimmune diseases. They function by inhibiting the activity of the $Ca^{2+}$/calmodulin-dependent phosphatase calcineurin toward nuclear factor of activated T-cells (NF-AT) in T-lymphocytes. However, use of CsA is associated with more serious side effects and worse clinical outcomes than FK506. Here we show that CsA, but not FK506, causes activation of the integrated stress response (ISR), an event which is normally an acute reaction to various types of intracellular insults, such as nutrient deficiency or endoplasmic reticulum stress. These effects of CsA involve at least two of the stress-activated protein kinases (GCN2 and PERK) that act on the translational machinery to slow down protein synthesis via phosphorylation of the eukaryotic initiation factor (eIF) 2$\alpha$ and thereby induce the ISR. These actions of CsA likely contribute to the adverse effects associated with its clinical application.**

Cyclosporin A (CsA) is a well-established antibiotic and immunosuppressant, used in a wide range of clinical settings, including treatment of autoimmune diseases (1), often to prevent graft rejection in organ transplant recipients (2), and as therapy for lysosomal storage diseases (3, 4). The primary mechanism by which CsA functions is by forming a complex with cyclophilin D, which in turn binds to and inhibits the activity of calcineurin, a $Ca^{2+}$/calmodulin-dependent phosphatase. CsA acts as an immunosuppressant by inhibiting the activity of calcineurin toward nuclear factor of activated T-cells (NF-AT) in T-lymphocytes. This impairs the translocation of NF-AT to the nucleus and consequently the transcription of genes for immunomodulatory factors, in particular interleukin 2 (IL-2) which is required for full T-cell activation (5). FK506 (also termed tacrolimus) is another structurally unrelated calcineurin inhibitor and immunosuppressant.

FK506 binds to a different immunophilin, FKBP12 (6), and may also exert additional effects independently of calcineurin (7). For instance, with respect to liver transplantation, FK506 is superior to CsA in improving survival (of patient and graft) and preventing acute rejection after liver transplantation but is also reported to increase the risk of posttransplant diabetes mellitus (8). Although the complications arising from immunosuppression are an anticipated outcome of their use, other potential side effects of calcineurin inhibitors must be considered in clinical practice, particularly with respect to their nephrotoxicity (9, 10).

In yeast, the phosphatase calcineurin also dephosphorylates and thereby inhibits the protein kinase Gcn2 (general control nondepressible 2), orthologous to mammalian GCN2 (11), which phosphorylates eukaryotic initiation factor 2 (eIF2), a key component of the protein synthesis machinery. Indeed, another study (12) showed that, in yeast, FK506 activates Gcn2, further supporting the notion that inhibition of calcineurin promotes activation of Gcn2 (11). Physiologically, GCN2 is activated upon amino acid starvation, which is signaled through the accumulation of uncharged tRNAs that in turn bind to and activate GCN2 (13–15). GCN2 phosphorylates the $\alpha$-subunit of eIF2 at serine 51 (Ser-51) (16), thus inhibiting the activity of eIF2's guanine nucleotide-exchange factor, eIF2B, and the translation of almost all mRNAs (17). However, translation of a subset of mRNAs, such as that for activating transcription factor (ATF) 4, is increased as an indirect consequence of eIF2$\alpha$ phosphorylation. ATF4 is pivotal to the integrated stress response (ISR), a process that is evoked by multiple stress stimuli, as ATF4 directly or indirectly activates genes required for cellular adaptation to stress, such as those involved in autophagy and resulting cell recovery. However, if the stress is prolonged, the ISR can promote apoptosis (18).

Gcn2 is the only eIF2$\alpha$ kinase in yeast, whereas in mammals there are three other eIF2 kinases (19). Expression of two of these enzymes is restricted to certain cells or conditions: protein kinase R, which is induced by type I interferons and activated by dsRNA during viral infection, and the heme-regulated eIF2$\alpha$ kinase (HRI), which signals iron deficiency in erythroid cells and is activated under conditions of lack of heme (18). The third, rather widely expressed, kinase is protein kinase R–like endoplasmic reticulum kinase (PERK), which is activated as a consequence of stress in the endoplasmic reticulum (ER), such as that elicited by the accumulation of unfolded or misfolded proteins or by perturbations in the levels of certain ions in the ER lumen (18).

This contrast between yeast and mammalian cells is of interest with respect to the use of calcineurin inhibitors for

This article contains supporting information.

* For correspondence: Christopher G. Proud, Christopher.proud@sahmri.com.

immunosuppression, as several research groups have observed an association between CsA administration and increases in PERK levels but not GCN2. An increase in total PERK was observed in RPTEC/TERT1 human renal epithelial cells upon CsA treatment (20). Furthermore, in cervical cancerous SiHa cells, CsA induced an increase in total PERK, with a modest change in its electrophoretic migration suggesting its increased phosphorylation (21). In glioma cells, an increase in phospho-PERK (indicating its activation) was observed upon CsA treatment (22). It must be noted, however, that GCN2 was not investigated in those studies. Nonetheless, these data collectively suggest a possible connection between CsA and induction of the ISR in mammalian cells, in addition to the link to GCN2 reported in yeast.

In this study, we examined whether calcineurin inhibitors promote the ISR in human and murine cells and identify the eIF2$\alpha$ kinases involved. We show that, surprisingly, GCN2 can also be activated by CsA and contributes to CsA's induction of the ISR. Furthermore, in stark contrast, FK506 does not elicit these effects on eIF2$\alpha$ phosphorylation or the ISR. Our data thus provide further insights into the distinct effects of these agents and a better understanding about the likely basis of differences in clinical toxicity.

## Results

### *CsA induces the ISR*

To assess whether, as occurs in yeast, inhibition of calcineurin could elicit activation of eIF2 kinases, we first examined the effect of the calcineurin inhibitors CsA and FK506 on eIF2$\alpha$ phosphorylation compared with brefeldin A (BFA), a known inducer of the ISR and ER stress (23, 24). To that end, the human cervical cancer HeLa and human lung carcinoma A549 cells were treated with DMSO, BFA, or either of the calcineurin inhibitors CsA or FK506 for 6 h prior to analysis of lysate samples by immunoblotting. In a similar fashion to BFA, CsA induced the phosphorylation of eIF2$\alpha$ at serine 51 (eIF2$\alpha$ P–Ser-51) (Fig. 1*A*) but FK506 did not. When phosphorylated on its $\alpha$-subunit, eIF2 inhibits the activity of its own guanine nucleotide exchange factor, eIF2B (17). Although this event inhibits general protein synthesis, it actually leads to enhanced translation of the mRNA encoding the transcription factor ATF4 (17, 18). Consistent with the increased phosphorylation of eIF2$\alpha$ P–Ser-51, CsA also increased the levels of the ATF4 protein, albeit not to the same extent as BFA (Fig. 1*A*). In contrast, FK506 had no effect on ATF4 protein levels, in line with its lack of effect on eIF2$\alpha$ phosphorylation.

To examine the effect of CsA and permit comparison with an alternative inducer of the ISR (thapsigargin, TPG), HeLa or A549 cells were exposed to BFA, CsA, or TPG for 6 h (Fig. 1*B*). In both lines, CsA induced increased eIF2$\alpha$ phosphorylation as did BFA and TPG. In summary, whereas CsA (similar with BFA or TPG) evoked the phosphorylation of eIF2$\alpha$ and the ISR in both cell lines tested, FK506 did not.

The compound ISRIB counters the inhibition of eIF2B by phosphorylated eIF2$\alpha$, and thus its downstream effects (25). HeLa and A549 cells were treated with BFA or CsA, with or without ISRIB, prior to analysis of separate sets of lysates by immunoblotting or by qPCR. ISRIB attenuated the induction of ATF4 by BFA and CsA in both cell lines (Fig. 2*A*). Additionally, ISRIB increased the phosphorylation of eIF2$\alpha$, likely because GADD34, a targeting subunit for the phosphatase that acts on phosphorylated eIF2$\alpha$, is normally up-regulated by increased ATF4 levels (26) and is thus itself inhibited by ISRIB. Finally, ATF4 drives transcription of multiple genes, including those encoding CCAAT-enhancer–binding protein homologous protein (*CHOP*, also a transcription factor) (27) and the CHOP/ATF4 target Tribbles homologue 3 (*TRB3*) (27), among others (28). Both mRNAs were markedly induced by BFA or CsA, and, as expected, these effects were reduced by ISRIB, and significantly with respect to TRB3 in HeLa cells and CHOP in A549 cells (Fig. 2*B*).

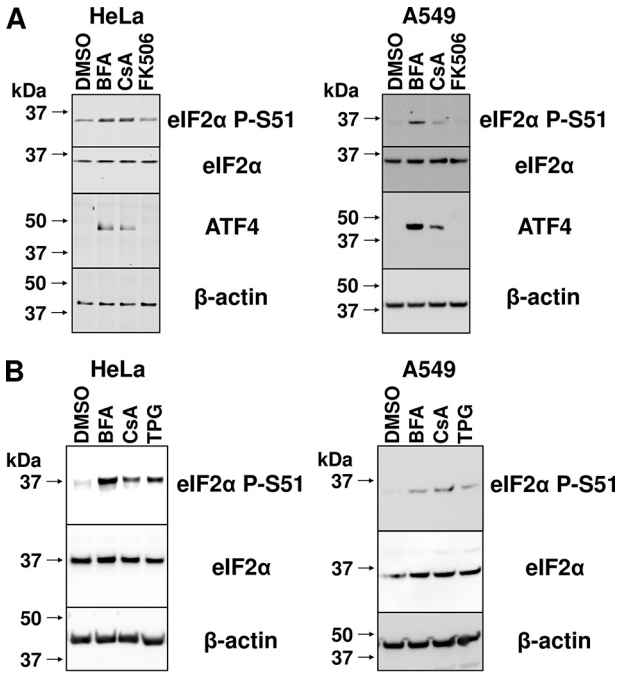


**Figure 1. CsA increases levels of ATF4 protein and activity.** *A*, protein extracts from HeLa and A549 cells treated with 1:500 DMSO, 5 $\mu$M BFA, 10 $\mu$M CsA, or 2 $\mu$M FK506 for 6 h were immunoblotted with the indicated antibodies. *B*, protein extracts from HeLa and A549 cells treated with 1:1000 DMSO, 5 $\mu$M BFA, 10 $\mu$M CsA, or 1 $\mu$M TPG for 6 h were immunoblotted with the indicated antibodies. All results are representative of three independent experiments.

We also employed mouse embryonic fibroblasts (MEFs) in which the sole phosphorylation site in eIF2$\alpha$ (Ser-51) (16) had been changed to alanine to preclude phosphorylation and its downstream consequences (eIF2$\alpha^{S51A/S51A}$) (29). These cells (in addition to control MEFs) were treated with CsA for 2, 6, or 16 h. At each time point, CsA caused the up-regulation of ATF4 in WT MEFs (Fig. S1), whereas no increase in ATF4 was seen in the eIF2$\alpha^{S51A/S51A}$ cells. Therefore, as expected, the phosphorylation of eIF2$\alpha$ is required for CsA's ability to promote the ISR, as assessed by induction of ATF4, excluding the possibility that CsA acts via other mechanisms to bring about the ISR.

In summary, consistent with BFA and TPG, CsA induced a classic stress response involving phosphorylation of eIF2$\alpha$, up-regulation of the expression of ATF4, and induction of ATF4-target genes.

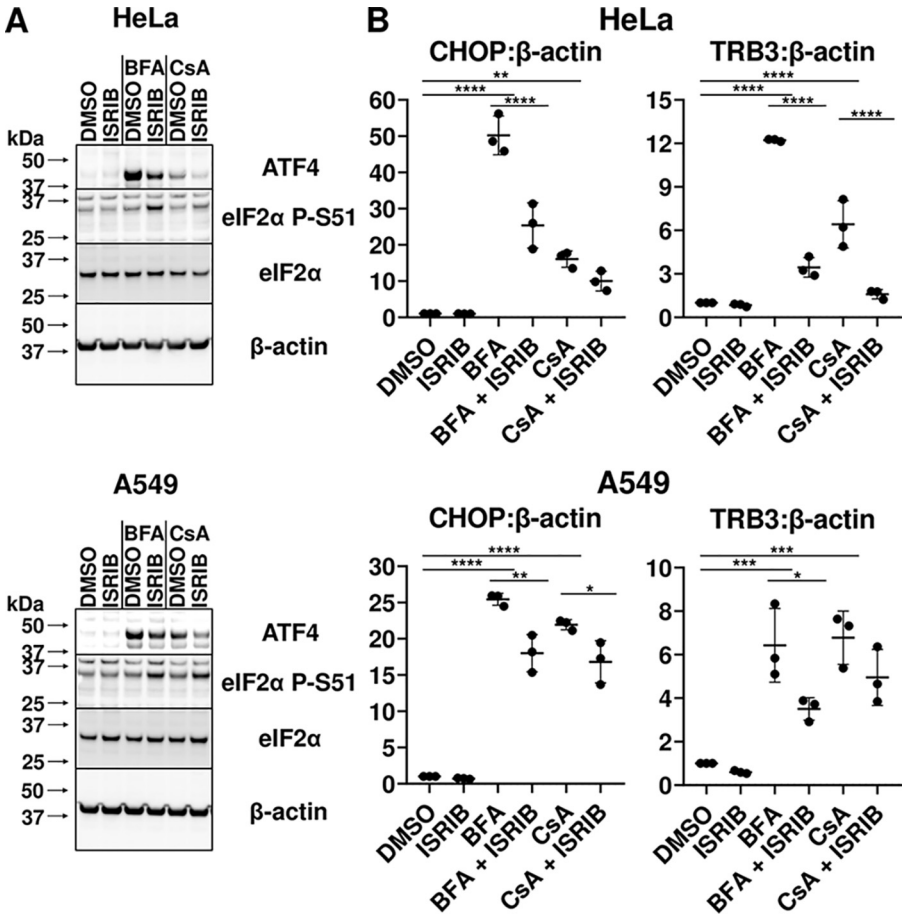


**Figure 2. ISRIB inhibits the up-regulation ATF4 by CsA.** *A*, protein extracts from HeLa and A549 cells treated with 1:1000 DMSO, 5 $\mu$M BFA or 10 $\mu$M CsA for 6 h, with or without 2 $\mu$M ISRIB, were immunoblotted using the indicated antibodies. Results are representative of three independent experiments. *B*, total RNA was extracted from similarly treated HeLa and A549 cells for evaluation via qPCR, employing primers designed to amplify fragments of the coding sequences of *CHOP* and *TRB3* and the internal control (*β*-actin). The data are the mean of the three biological replicates. *Error bars* represent ± S.D. Significance was evaluated using two-way ANOVA. ANOVA summary for CHOP amplification in HeLa cells: Interaction F = 18.79 (2, 12), interaction *P* value = 0.0002; row factor F = 158.2 (2, 12), row factor *P* value < 0.0001; column factor F = 35.72 (1, 12), column factor *P* value < 0.0001. ANOVA summary for TRB3 amplification in HeLa cells: Interaction F = 51.84 (2, 12), interaction *P* value < 0.0001; row factor F = 133.2 (2, 12), row factor *P* value < 0.0001; column factor F = 175.1 (1, 12), column factor *P* value < 0.0001. ANOVA summary for CHOP amplification in A549 cells: Interaction F = 7.354 (2, 12), interaction *P* value = 0.0082; row factor F = 288.8 (2, 12), row factor *P* value < 0.0001; column factor F = 30.32 (1, 12), column factor *P* value = 0.0001. ANOVA summary for TRB3 amplification in A549 cells: Interaction F = 2.271 (2, 12), interaction *P* value = 0.1458; row factor F = 41.77 (2, 12), row factor *P* value < 0.0001; column factor F = 12.63 (1, 12), column factor *P* value = 0.004. For clarity, not all the significant differences are indicated.

### *Both GCN2 and PERK contribute to induction of the ISR by CsA*

As mentioned in the Introduction, several studies have indicated that CsA activates PERK (20–22), whereas in yeast, it has been demonstrated that calcineurin inhibition leads to activation of GCN2 (11). On the other hand, our data (Fig. 1) demonstrate that an alternative inhibitor of calcineurin (FK506) does not activate the ISR. To assess the involvement of these two kinases in the induction of the ISR upon CsA treatment, WT, GCN2$^{-/-}$ (30), or PERK$^{-/-}$ (31) MEFs were treated with DMSO, BFA, CsA, or histidinol for 6 h (Fig. 3*A*). (Histidinol is an amino alcohol that inhibits the activity of the histidyl-tRNA synthetase, leading to the accumulation of uncharged tRNA$^{His}$ and consequent activation of GCN2.) As expected, upon BFA treatment of either WT or GCN2$^{-/-}$ MEFs, we observed a shift in the electrophoretic migration of PERK, indicative of its phosphorylation and thus its activation. In both cell lines, the activation of PERK was associated with a similar increase in ATF4 protein levels. As expected, in PERK$^{-/-}$ MEFs no significant increase in ATF4 was observed after BFA treatment (Fig. 3*A*). Reciprocally, histidinol treatment induced the phosphorylation of GCN2 and increased ATF4 expression only in WT and PERK$^{-/-}$ MEFs. As judged by the mobility shift, CsA evoked activation of PERK in WT and GCN2$^{-/-}$ MEFs (Fig. 3*A*), in line with earlier indications from glioma cells (22). However, the shift appeared less pronounced with CsA treatment than with BFA.

The key observation here is that in PERK$^{-/-}$ (or GCN2$^{-/-}$) MEFs, as in WT cells, CsA increases ATF4 protein levels (Fig. 3*A*). This indicates that PERK is not the only kinase that contributes to the increase in the level of ATF4 protein caused by CsA, although it is noticeable that the increase in ATF4 upon CsA treatment was lower in GCN2$^{-/-}$ MEFs than in the two other genotypes. Although we failed to observe a significant increase in the phosphorylation of GCN2 in response to CsA, this observation does suggest a significant role of GCN2 in the induction of ATF4 protein by CsA. Intriguingly, in PERK$^{-/-}$ cells, we observed a very marked increase in the levels of phosphorylated GCN2, even under basal conditions (Fig. 3*A*). Moreover, it points to a potential compensatory mechanism between

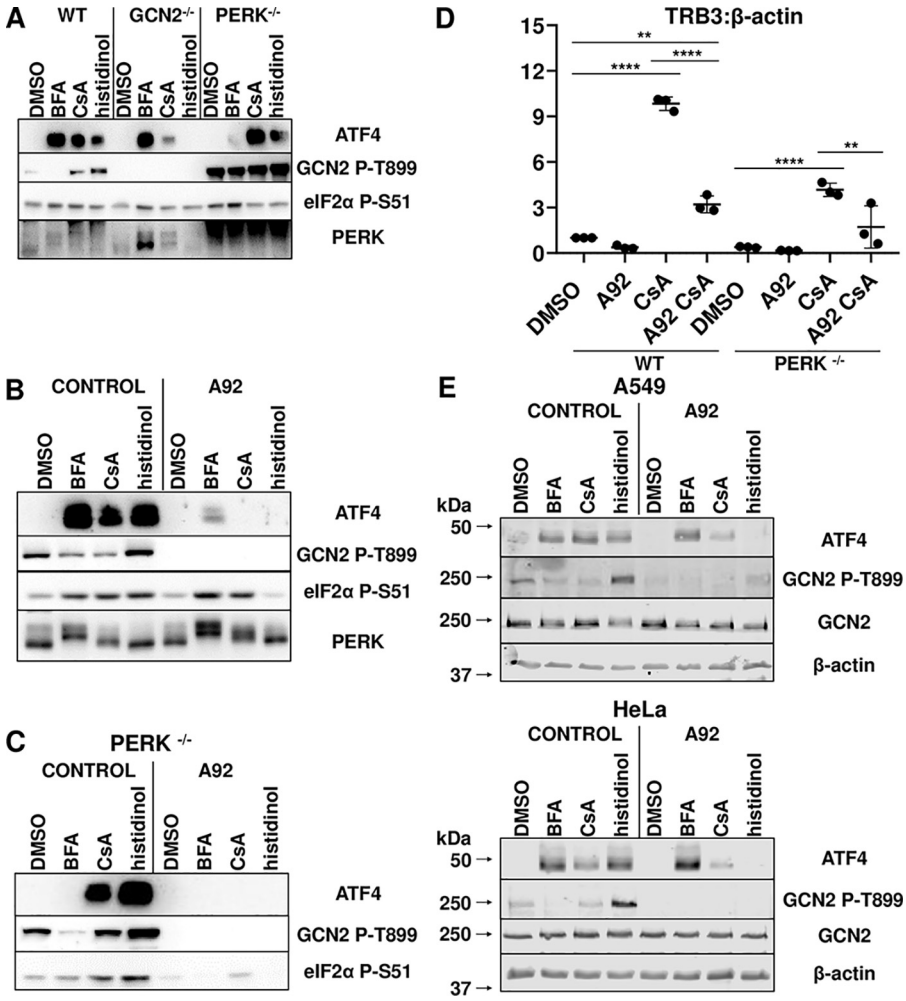


**Figure 3. CsA mediated up-regulation of ATF4 requires the eIF2α kinases GCN2 or PERK.** *A*, protein extracts from WT, GCN2$^{-/-}$, and PERK$^{-/-}$ MEFs that had been treated for 6 h with 1:1000 DMSO, 5 $\mu$M BFA, 10 $\mu$M CsA, or 2 mM histidinol were analyzed by immunoblotting with the indicated antibodies. *B*, protein extracts from WT MEFs treated for 6 h with 1:1000 DMSO, 5 $\mu$M BFA, 10 $\mu$M CsA, or 2 mM histidinol, with or without additional treatment with 5 $\mu$M A92, were immunoblotted with the indicated antibodies. *C*, protein extracts from PERK$^{-/-}$ MEFs treated for 6 h with 1:1000 DMSO, 5 $\mu$M BFA, 10 $\mu$M CsA, or 2 mM histidinol, with or without additional treatment with 5 $\mu$M A92 were immunoblotted with the indicated antibodies. *D*, total RNA was extracted from WT, GCN2$^{-/-}$, and PERK$^{-/-}$ MEFs that had been treated for 6 h with 1:1000 DMSO or 10 $\mu$M CsA with or without additional treatment with 5 $\mu$M A92 and then evaluated via qPCR, employing primers designed to amplify fragments of the coding sequences of TRB3 and the internal control ($\beta$-actin). *Error bars* represent ± S.D. Significance was evaluated using two-way ANOVA. ANOVA summary: Interaction F = 28.24 (3, 16), interaction *P* value < 0.0001; row factor F = 71.61 (1, 16), row factor *P* value < 0.0001; column factor F = 170.6 (3, 16), column factor *P* value < 0.0001. For clarity, not all the significant differences are indicated. *E*, protein extracts from A549 and HeLa cells treated for 6 h with 1:1000 DMSO, 5 $\mu$M BFA, 10 $\mu$M CsA, or 2 mM histidinol, with or without additional treatment with 5 $\mu$M A92, were immunoblotted with the indicated antibodies. All results are shown as the mean of the three biological replicates.

the two kinases whereby the absence of one influences the other, a phenomenon that has previously been observed in GCN2-KO mice (32). In support of this, we also observed a large increase in total PERK protein levels in eIF2$\alpha^{S51A/S51A}$ cells (Fig. S1). Further work focusing on the effects of CsA is required to unravel the mechanisms involved.

The above data clearly show that CsA induces the phosphorylation of eIF2$\alpha$, an effect which can inhibit general protein synthesis. To assess the effect of CsA on protein synthesis we utilized the nonradioactive SUnSET method (33), in which incorporation of puromycin into newly made proteins is assessed in a quantitative way by analyzing cell lysates by immunoblot. As shown in Fig. S2, as expected, BFA and histidinol each inhibited puromycin incorporation over a 4-h treatment period. The effect of BFA was attenuated in eIF2$\alpha^{S51A/S51A}$ cells (Fig. S2), consistent with it being largely because of phosphorylation of eIF2. The effect of histidinol was still evident in eIF2$\alpha^{S51A/S51A}$ cells, likely because this agent actually causes depletion of the level of histidinyl-tRNAs, which are essential for protein synthesis, so that it still inhibits this process in the knock-in cells. The weaker effect of CsA was also retained in eIF2$\alpha^{S51A/S51A}$ MEFs. Taken together, these data indicate that CsA does inhibit protein synthesis and that, although this effect is weaker than that of, *e.g.* BFA, it still suffices to induce ATF4. Importantly, the data also imply that CsA affects protein synthesis through additional mechanisms, not only via eIF2 phosphorylation; further work is needed to study the mechanisms involved in this.

### *An inhibitor of GCN2 blunts the effects of CsA*

To validate a potential role for GCN2 in the effects of CsA, we made use of A92, a recently developed inhibitor of this

kinase (34). As shown in Fig. 3*B*, A92 efficiently inhibited the phosphorylation of GCN2 and the induction of the expression of ATF4 following histidinol treatment in WT MEFs, confirming its efficacy. Remarkably, A92 also abolished the induction of ATF4 expression caused by CsA. One unexpected observation was that A92 decreased ATF4 levels in BFA-treated cells, which might, in principle, be explained by a nonspecific effect of A92 on PERK activity. Nevertheless, no effect of A92 was observed on the modest mobility shift of PERK under the different treatment conditions (Fig. 3*B*), suggesting it does not affect PERK. To exclude a possible effect of A92 on PERK confounding our interpretation of the CsA data, we repeated the experiment in PERK$^{-/-}$ MEFs. In these cells, we also observed that A92 abolished the increase in ATF4 expression caused by CsA (Fig. 3*C*), confirming that the inhibitory effect of A92 on the regulation of ATF4 by CsA is not because of interference with PERK. Finally, we also tested the impact of A92 on the level of expression of the ATF4 target gene *TRB3*. Following treatment with CsA for 6 h, we observed a significant increase in *TRB3* mRNA, which was significantly diminished by A92 treatment in accordance with the lower levels of ATF4 shown in Fig. 3*B*. The results of a similar experiment with PERK$^{-/-}$ MEFs were comparable to those observed in WT MEFs, in that CsA induced an increase in TRB3 mRNA, and A92 significantly reduced this increase (Fig. 3*D*). Overall, these data demonstrate that, in addition to activating PERK, CsA treatment can stimulate GCN2 and thus the expression of ATF4 (as well as the induction of at least one of its target genes, *TRB3*). Furthermore, in both human cancer cells lines tested (HeLa and A549), A92 again strongly inhibited the induction of ATF4 by CsA (Fig. 3*E*). These data further show that GCN2 contributes to the effects of CsA on ATF4, *i.e.* the induction of the ISR.

### *CsA does not induce the ISR by inhibiting calcineurin*

Previous data (12) have shown that FK506 can induce the activation of Gcn2 in yeast (35). However, our data from A549 cells (Fig. 1*A*) show that FK506, unlike CsA, did not induce phosphorylation of eIF2$\alpha$ or up-regulation of the ATF4 protein. In additional experiments, FK506 did not elicit the ISR in HeLa cells (Fig. 4*A*), in contrast to CsA, as demonstrated by its failure to increase ATF4 protein (Fig. 4*A*) or CHOP mRNA (Fig. 4*B*) levels in both lines. Importantly, these data imply that inhibition of calcineurin is not the mechanism by which CsA induces the ISR.

In view of the lack of effect of FK506 on eIF2$\alpha$ phosphorylation and related responses, it was relevant to verify its efficacy confirming its ability to compete with rapamycin for binding to their common partner, the immunophilin FKBP12, because the rapamycin–FKBP12 complex inhibits the function of the mTOR complex 1 (mTORC1). Although the FK506-FKBP12 complex does not, FK506 can alleviate such inhibition and restore mTORC1 signaling (36). HeLa cells were therefore exposed to a range of rapamycin concentrations (100 to 1 nM), with or without co-treatment with FK506. mTORC1 signaling was then evaluated by immunoblotting for phosphorylated ribosomal protein (rp) S6; this is an indirect target of mTORC1, because rpS6 is phosphorylated at serines 240 and 244 (P–Ser-240/244) by p70S6K, which is itself activated by phosphorylation at threonine 389 by mTORC1 (37, 38). Rapamycin eliminated phosphorylation of rpS6 P–Ser-240/244, even at 1 nM, and this inhibition of mTORC1 signaling was, as expected, alleviated by FK506 (Fig. 4*C*), thus demonstrating its efficacy.

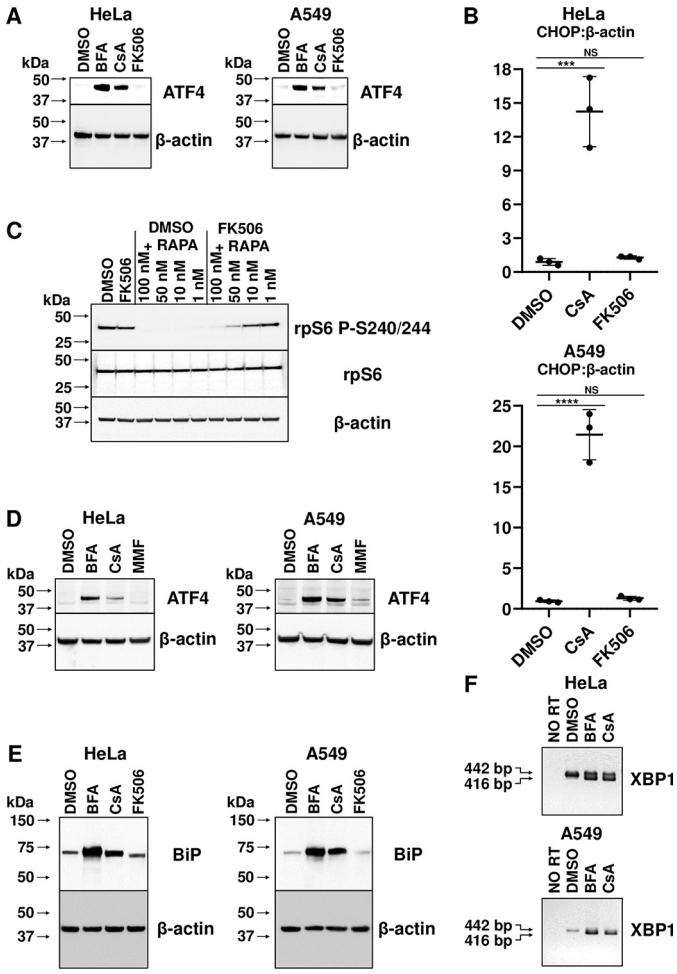


**Figure 4. The calcineurin inhibitor FK506 does not increase ATF4 protein or activity, whereas CsA induces markers of ER stress.** *A*, protein extracts from HeLa and A549 cells that had been treated with 1:500 DMSO, 5 $\mu$M BFA, 10 $\mu$M CsA, or 2 $\mu$M FK506 for 24 h were immunoblotted with antibodies to ATF4 and $\beta$-actin. *B*, total RNA was extracted from HeLa and A549 cells that had been treated with 1:500 DMSO, 10 $\mu$M CsA, or 2 $\mu$M FK506 for 24 h for evaluation via qPCR, employing primers designed to amplify fragments of the coding sequences of *CHOP* and the internal control ($\beta$-actin). *Error bars* represent $\pm$ S.D. Significance was evaluated using one-way ANOVA. ANOVA summary for HeLa cells: F = 53.01, *P* value = 0.0002. ANOVA summary for A549 cells: F = 129, *P* value $<$ 0.0001. *C*, protein extracts from HeLa cells treated for 6 h with 1:500 DMSO or 2 $\mu$M FK506 with or without additional treatments with the indicated concentrations of rapamycin (*RAPA*) were immunoblotted with antibodies for total and phospho (P)-rpS6 (P–Ser-240/244) and $\beta$-actin. Results are representative of two independent experiments. *D*, protein extracts from HeLa and A549 cells treated with 1:1000 DMSO, 5 $\mu$M BFA, 10 $\mu$M CsA, or 2.5 mM monomethyl fumarate (*MMF*) for 24 h were immunoblotted with antibodies to ATF4 and $\beta$-actin. Results are representative of two independent experiments. *E*, protein extracts from A549 cells that had been treated with 1:1000 DMSO, 5 $\mu$M BFA, 10 $\mu$M CsA, or 2 $\mu$M FK506 for 6 h were immunoblotted with the indicated antibodies. Results are representative of two independent experiments. *F*, total RNA was extracted from HeLa and A549 cells treated with 1:1000 DMSO, 5 $\mu$M BFA, or 10 $\mu$M CsA for 6 h. This was used as a template for the preparation of cDNA, which was analyzed by qualitative PCR, employing primers (42) designed to amplify full-length (442 bp) and IRE1-processed (416 bp) fragments of the coding sequences of XBP1. All results are represented as the mean of the three biological replicates, unless otherwise stated.

### CsA does not appear to induce the ISR through mitochondrial stress

Given that our data suggest that CsA may exert its effects independently of inhibiting calcineurin (otherwise FK506 would elicit similar reactions) our attention was drawn to another binding partner for CsA, cyclophilin D. Cyclophilin D forms part of the mitochondrial permeability transition pore whose opening enhances the permeability of the mitochondrial membrane and is associated with induction of mitochondrial stress (39). We speculated that CsA may exert its effects on the ISR by binding to and ablating cyclophilin D functions. To mimic this effect of CsA without using that compound, we performed siRNA-mediated knockdown of *CYPD*. However, this caused no reproducible change in the modulation of ATF4 protein (Fig. S3), indicating that impairment of cyclophilin D function does not induce the ISR.

The ISR has recently been suggested to be a consequence of the mitochondrial stress response in mammals. The enzyme implicated in this effect (40) is mitochondrial fumarate hydratase (encoded by the *FH* gene in humans), which catalyzes the conversion of fumarate to L-malate. It was shown that either knockdown of this mRNA or treatment of cells with monomethyl fumarate (to simulate the increase in fumarate resulting from reduced *FH* expression or function) increased the expression of *ATF4* and *CHOP* (40). To assess whether CsA could be inducing the ISR by causing mitochondrial stress and, in turn, interfering with fumarate hydratase, we repeated the latter experiment. Interestingly, however, in our hands supplementing the cells' growth medium with monomethyl fumarate did not itself elicit the expected increase of ATF4 protein in either HeLa or A549 cells, unlike BFA or CsA (Fig. 4*D*). Finally, to assess further the possibility that CsA-induced mitochondrial stress accounts the activation of the ISR, ATP levels were measured using the CellTiter-Glo® Luminescent Cell Viability Assay. If CsA induced mitochondrial stress in our experiments, reduced ATP levels would be anticipated. Data were normalized to the number of viable cells as determined by calcein AM staining subsequent to treatment with vehicle, CsA, or FK506. However, according to this assay, they were not significantly altered by either CsA or FK506 (Fig. S4). Thus, collectively, our data do not indicate that CsA induces the ISR through mitochondrial stress.

### CsA also activates the IRE1 arm of the unfolded protein response

Immunoblotting of A549 and HeLa cells treated with either BFA, CsA, or FK506 to detect BiP/grp78 demonstrated that CsA (like BFA), but not FK506, increased the expression of BiP, a chaperone protein which functions in the ER, indicating that it elicits an ER stress response in these cell lines (Fig. 4*E*). Indeed, in addition to activating PERK, ER stress also affects the splicing of the mRNA encoding XBP1, a transcription factor that plays an important role in the unfolded protein response (which in turn is triggered by ER stress) (35) and whose activation involves splicing of the coding sequence of its mRNA by IRE1 (41). To study this, total RNA was extracted from HeLa and A549 cells that had been treated with DMSO, BFA, or CsA for 6 h and then analyzed by qualitative RT-PCR employing primers designed to amplify full-length (442 bp) and IRE1-processed (416 bp) fragments of the coding sequence of XBP1 (42). In both lines, both BFA and CsA treatment increased splicing of the XBP1 RNA, again indicating activation of the unfolded protein response (Fig. 4*F*).

## Discussion

Our data indicate that the calcineurin inhibitor CsA activates both GCN2 and PERK in mammals (Fig. 5). However, strikingly, FK506 did not elicit the same effects, which strongly implies that inhibition of calcineurin itself is not responsible for the effects of CsA on these kinases.

As mentioned previously, associations between calcineurin activity and ISR inhibition have been suggested by studies in both yeast and vertebrates. With respect to the former, calcineurin's phosphatase activity has been implicated in the inhibition of Gcn2 (11). Additionally, several research groups have previously observed increases in total and/or phospho-PERK levels (and, by implication, ER stress) following administration of the calcineurin inhibitor CsA (20–22), although no mechanistic information was provided and other eIF2 kinases were not examined.

Physiologically, GCN2 is activated consequent to reduced intracellular amino acid levels via binding of uncharged tRNA (15). It is possible that CsA interacts directly with GCN2 in a similar way to that of uncharged tRNA. Recently, an inhibitor of GCN2 (termed A92) has been developed (34), and we have demonstrated that this inhibited the effect of CsA on the ISR in a range of cell lines (Fig. 3, *B–E*)

On the other hand, the ability of CsA to activate PERK seems unlikely to be because of a specific direct effect on PERK itself, as CsA also induced another arm of the unfolded protein response, *i.e.* the altered splicing of XBP1 (Fig. 4, *E* and *F*). Indeed, the up-regulation of the ER-localized chaperone BiP/grp78 (an activator of both PERK and XBP1 splicing, which is up-regulated upon ER stress) potentially implies an ability for CsA to interfere with BiP/grp78. This suggests that CsA promotes ER stress or a related process. Indeed, some previous reports have hinted at effects of CsA (but not FK506) on ER stress, as indicated by increased expression of the ER proteins BiP/GRP78 and IRE1$\alpha$, alongside cellular vacuolation in cervical cancer SiHa cells (21). The authors concluded that the differing effects were not because of inhibition of calcineurin, which is consistent with our observations that they are not evoked by FK506. Furthermore, CsA, which has also been implicated in posttransplantation diabetes mellitus (8), has been shown to promote XBP1 splicing in pancreatic $\beta$-cells, although interestingly neither ATF4 nor BiP/grp78 was affected (43). Finally, certain ER proteins are also reported to be elevated in children who had received CsA and developed nephrotic syndrome (44), supporting potential clinical relevance of our findings. Our data imply that proteins induced by ER stress may be valuable as biomarkers of CsA toxicity. Our data also imply that CsA inhibits protein synthesis by additional mechanisms, not only by inducing the phosphorylation of eIF2$\alpha$.

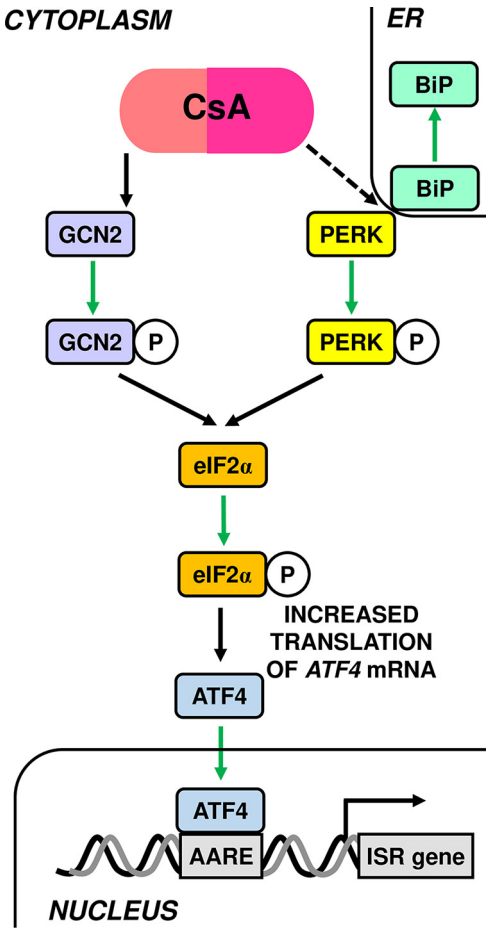


**Figure 5.** CsA activates both GCN2 and PERK in mammalian cells.

An unexpected outcome of this work was the observations made in derivatives of MEFs where either PERK or GCN2 had been removed, or where the regulatory phosphorylation site in eIF2$\alpha$ (Ser-51) has been mutated. In PERK$^{-/-}$ cells, we observed a large increase in the levels of phosphorylated GCN2 (Fig. 3*A*), whereas in eIF2$\alpha^{S51A/S51A}$ cells there was a dramatic increase in total PERK protein levels, even under basal conditions (Fig. S1). This indicates novel, uncharacterized links between these components of the ISR, whereby the absence of one of them may cause increases in another, perhaps as a feedback mechanism to compensate for the deficiency. Not only does this indicate bidirectional crosstalk through the ISR pathway, but also suggests that even in normal conditions, there is a basal level of ISR activity which, no matter how low, is still crucial to cellular function. This should form the basis of future studies.

In summary, the major findings of our study include the first evidence that CsA can evoke increased phosphorylation of eIF2$\alpha$ and downstream ISR through either GCN2 *or* PERK. Furthermore, although both act as immunosuppressants by inhibiting calcineurin activity, our data demonstrate that CsA elicits eIF2-mediated stress responses in mammalian cells but FK506 does not. This strongly suggests that CsA's mode of action in these phenomena is not by inhibiting calcineurin. Importantly, as FK506 does not activate these stress responses, this difference likely helps to explain its lesser side effects as compared with CsA, resulting in better tolerance and outcomes in patients who have undergone transplant surgery.

## Experimental procedures

### *Chemicals for cell treatments*

All chemicals were purchased from Sigma-Aldrich. Brefeldin A (BFA), rapamycin, CsA, FK506, thapsigargin (TPG), and ISR inhibitor (ISRIB, *i*ntegrated *s*tress *r*esponse *i*nhi*b*itor) (25) were each dissolved in DMSO, while histidinol dihydrochloride, puromycin, and monomethyl fumarate were prepared in Milli-Q water.

### *Cell culture*

A549 cells derived from cancerous lung tissue, HeLa cells derived from cervical cancer cells, and all genotypes of mouse embryonic fibroblasts were maintained in Dulbecco's modified Eagle's medium with 10% (v/v) fetal bovine serum (Life Technologies) and 100 units/ml penicillin/streptomycin (Sigma-Aldrich) and incubated at 37°C and 5% (v/v) $CO_2$.

### *RNA extraction*

Cells grown in 6-well plates were washed using 2 ml PBS, followed by the addition of 500 $\mu$l TRIzol Reagent (Thermo Fisher). Total RNA was then prepared according to the manufacturer's instructions and provided a template for complementary DNA (cDNA) preparation.

### *Qualitative RT-PCR*

cDNA was first synthesized from total RNA using the SuperScript III First-Strand Synthesis System (Life Technologies). Fifty $\mu$l reactions were prepared using cDNA (prepared with 6.25 ng starting RNA), 100 nM forward and reverse primers, 1 unit HotStarTaq DNA polymerase, 1× Q-solution, 1 mM $MgCl_2$, 200 $\mu$M dNTP mix, and Milli-Q water. Reactions were performed at 95°C for 15 min; 35 times (94°C for 1 min; 60°C for 1 min; 72°C for 1 min); 72°C for 10 min. Previously published oligonucleotide primers (42) were employed to amplify a portion of the coding sequence of XBP1 and flanking the 26 nucleotides removed by IRE1.

### *Quantitative real time PCR (qPCR)*

cDNA was first prepared from total RNA using the SuperScript III First-Strand Synthesis System (Life Technologies). Oligonucleotide primers designed to amplify fragments of the coding sequences of the genes of interest (Table 1) and the internal control, $\beta$-actin. To each well were added 0.84× SYBR Green Fast Mix (Applied Biosystems), 5–10 $\mu$l cDNA (6.25–12.5 ng starting RNA), 200 nM forward and reverse primers and Milli-Q water to 20 $\mu$l. qPCR reactions proceeded as follows on an ABI Step One Plus qPCR instrument (Applied Biosystems): 95°C for 20 s; 40 times (95°C for 3 s; 60°C for 30 s). The comparative threshold cycle protocol was employed to determine amounts of the target mRNA.

**Table 1**
**Oligonucleotides employed in this study for PCR**

| Gene | Accession | Human/Mouse | Forward (5′→3′) | Reverse (5′→3′) |
|---|---|---|---|---|
| CHOP | NM_004083.5 | H | CAGCTGAGTCATTGCCTTTC | TTGATTCTTCCTCTTCATTTCC |
| TRB3 | NM_021158.4 | H | GTATACCTGCAAGGTGTACC | AAAAAGGCGTAGAGGAGCTG |
| XBP1 (42) | NM_005080 | H | CCTTGTAGTTGAGAACCAGG | GGGGCTTGGTATATATGTGG |
| TRB3 | NM_175093.2 | M | CCAGAGATACTCAGCTCCCG | GAGGAGACAGCGGATCAGAC |
| β-actin | | | CTGGCACCACACCTTCTAC | GGGCACAGTGTGGGTGAC |

### *Immunoblotting*

Cells grown in 6-well plates were washed using 2 ml ice-cold PBS, then lysed with 100–300 μl RIPA buffer supplemented with 2.5 mM $Na_2H_2P_2O_7$ (Sigma-Aldrich), 1 mM β-glycerophosphate (Sigma-Aldrich), 1 mM $Na_3VO_4$ (Sigma-Aldrich), and 1× Protease Inhibitor mixture (Roche). Cells were then rocked for 30 min at 4°C, scraped, and transferred to a microcentrifuge tube. Cell suspensions were centrifuged at 15,871 × *g* for 30 min at 4°C, then the supernatant was maintained and transferred to new microfuge tubes. Protein concentration was quantified for sample normalization using the Lowry procedure (45).

Equal amounts (by protein) of samples were subjected to SDS-PAGE, then transferred to a nitrocellulose membrane. The membrane was blocked for ~90 min in PBS containing 0.1% Tween 20 and 2% (w/v) BSA at 4°C. Membranes were then rolled overnight at 4°C in the same solution supplemented with one of the following antibodies: 1/1000 rabbit polyclonal anti-ATF4 (Cell Signaling Technology); 1/1000 mouse monoclonal anti-eIF2α (Cell Signaling Technology); 1/1000 rabbit polyclonal anti-eIF2α P-S51 (Cell Signaling Technology); 1/1000 rabbit monoclonal anti-BiP (Cell Signaling Technology); rabbit monoclonal anti-GCN2 P-T899; 1/1000 (Abcam); 1/1000 rabbit monoclonal anti-GCN2 (Cell Signaling Technology); 1/5000 mouse monoclonal anti-puromycin clone 12D10 (Millipore), or 1/10000 mouse monoclonal anti–β-actin (Sigma-Aldrich). The following day, the membrane was washed three times for 5 to 10 min at room temperature in PBS containing 0.1% Tween 20, then incubated at room temperature for 1 h in PBS containing 0.1% Tween 20 and 2% BSA plus 1/3000 horseradish peroxidase–linked sheep anti-mouse (GE Healthcare), goat anti-rabbit (Millipore), or 1/5000 mouse anti-human β-actin (Sigma-Aldrich) IgG. The membrane was then washed three times for 5 to 10 min at room temperature in PBS with 0.1% Tween 20, drained, treated with the SuperSignal West Pico Plus Chemiluminescent Substrate (Thermo Fisher), developed on a LAS-4000 apparatus (Fujifilm), and analyzed using Multigauge 1D software (Fujifilm). In some cases, further densitometric quantification was implemented using ImageJ (National Institutes of Health).

### *CellTiter-Glo assay*

ATP levels of cells grown in 96-well plates were determined via the application of a CellTiter-Glo® Luminescent Cell Viability Assay and normalized to viable cell number as determined via calcein AM, according to the manufacturer's instructions (Promega).

### *Measure of protein synthesis by SUnSET*

SUnSET experiments were performed as described previously (33), briefly cells were treated with 5 μg/ml of puromycin during the last 30 min of the experiment. Then, the cells were harvested, and immunoblotting was performed using TGX FastCast Stain-Free Acrylamide 10% gel (Bio-Rad). Stain-free imaging allows for the normalization of the puromycin signal to the total protein on a blot.

### *Statistics*

Unless otherwise stated, immunoblotting and qualitative RT-PCR experiments were performed in biological triplicate. qPCR experiments were performed in biological triplicate, with each replicate analyzed in turn in technical triplicate. For data represented graphically, *error bars* represent ± S.D. of the indicated number of independent experiments performed. The specific test used to determine statistical significance is indicated in the relevant figure legend. Note: * = $p \leq 0.05$, ** = $p \leq 0.01$, *** $p = \leq 0.001$, **** $p = \leq 0.0001$.

## Data availability

All data of this publication have been contained within this manuscript or are available from the corresponding author (Chris Proud; SAHMRI, Adelaide, Australia; E-mail: Christopher.Proud@sahmri.com) upon reasonable request.

*Acknowledgments*—We are grateful to Dr. Xuemin Wang, Stuart De Poi, Roman Lenchine, and Lauren Sandeman (Lifelong Health Theme, SAHMRI) for advice and technical assistance. We thank Professor Terence Herbert (Lincoln, UK), Dr. Anne-Catherine Maurin (Clermont-Ferrand, France), Dr. Randal Kaufman (La Jolla, CA, USA), and Professor David Ron (Cambridge, UK) for providing MEFs from genetically modified mice.

*Author contributions*—A. O. F. and C. G. P. conceptualization; A. O. F., V. C., J. X., and J. A. investigation; A. O. F. and J. A. methodology; A. O. F. and C. G. P. writing-review and editing; V. C., J. A., and C. G. P. project administration; J. A. and C. G. P. writing-original draft; C. G. P. supervision; C. G. P. funding acquisition.

*Funding and additional information*—This work was supported by the Hopwood Centre for Neurobiology (to A. O. F. and C. G. P.), SAHMRI (to J. X. and C. G. P.), and the Institut National de Recherche pour l'Agriculture, l'Alimentation et l'Environnement (to V. C. and J. A.).

*Conflict of interest*—The authors declare that they have no conflicts of interest with the contents of this article.

*Abbreviations*—The abbreviations used are: CsA, cyclosporin A; FK506, tacrolimus; NF-AT, nuclear factor of activated T-cells; ISR, integrated stress response; eIF, eukaryotic initiation factor; ATF,

activating transcription factor; ER, endoplasmic reticulum; PERK, protein kinase R–like ER kinase; TPG, thapsigargin; MEF, mouse embryonic fibroblast; rp, ribosomal protein; BFA, brefeldin A; cDNA, complementary DNA; ANOVA, analysis of variance.

## References


1. Mieli-Vergani, G., Vergani, D., Czaja, A. J., Manns, M. P., Krawitt, E. L., Vierling, J. M., Lohse, A. W., and Montano-Loza, A. J. (2018) Autoimmune hepatitis. *Nat. Rev. Dis. Primers* **4,** 18017 CrossRef Medline
2. van den Bosch, T. P., Kannegieter, N. M., Hesselink, D. A., Baan, C. C., and Rowshani, A. T. (2017) Targeting the monocyte-macrophage lineage in solid. *Front. Immunol.* **8,** 153 CrossRef Medline
3. Dickson, P., Peinovich, M., McEntee, M., Lester, T., Le, S., Krieger, A., Manuel, H., Jabagat, C., Passage, M., and Kakkis, E. D. (2008) Immune tolerance improves the efficacy of enzyme replacement therapy in canine mucopolysaccharidosis I. *J. Clin. Invest.* **118,** 2868–2876 CrossRef Medline
4. Ponder, K. P. (2008) Immune response hinders therapy for lysosomal storage diseases. *J. Clin. Invest.* **118,** 2686–2689 CrossRef Medline
5. Bendickova, K., Tidu, F., and Fric, J. (2017) Calcineurin-NFAT signalling in myeloid leucocytes: New prospects and pitfalls in immunosuppressive therapy. *EMBO Mol. Med.* **9,** 990–999 CrossRef Medline
6. Abraham, R. T., and Wiederrecht, G. J. (1996) Immunopharmacology of rapamycin. *Annu. Rev. Immunol.* **14,** 483–510 CrossRef Medline
7. Mori, A., Suko, M., Kaminuma, O., Inoue, S., Ohmura, T., Hoshino, A., Asakura, Y., Terada, E., Miyazawa, K., Nosaka, C., Okumura, Y., Ito, K., and Okudaira, H. (1997) IL-2-induced IL-5 synthesis, but not proliferation, of human CD4+ T cells is suppressed by FK506. *J. Immunol.* **158,** 3659–3665 Medline
8. Haddad, E. M., McAlister, V. C., Renouf, E., Malthaner, R., Kjaer, M. S., and Gluud, L. L. (2006) Cyclosporin versus tacrolimus for liver transplanted patients. *Cochrane Database Syst. Rev.* **4,** CD005161 CrossRef Medline
9. Naesens, M., Kuypers, D. R., and Sarwal, M. (2009) Calcineurin inhibitor nephrotoxicity. *Clin. J. Am. Soc. Nephrol.* **4,** 481–508 CrossRef Medline
10. Wu, Q., and Kuca, K. (2019) Metabolic pathway of cyclosporine A and its correlation with nephrotoxicity. *Curr. Drug Metab.* **20,** 84–90 CrossRef Medline
11. Vlahakis, A., and Powers, T. (2014) A role for TOR complex 2 signaling in promoting autophagy. *Autophagy* **10,** 2085–2086 CrossRef Medline
12. Rodriguez-Hernandez, C. J., Sanchez-Perez, I., Gil-Mascarell, R., Rodriguez-Afonso, A., Torres, A., Perona, R., and Murguia, J. R. (2003) The immunosuppressant FK506 uncovers a positive regulatory cross-talk between the Hog1p and Gcn2p pathways. *J. Biol. Chem.* **278,** 33887–33895 CrossRef Medline
13. Dong, J., Qiu, H., Garcia-Barrio, M., Anderson, J., and Hinnebusch, A. G. (2000) Uncharged tRNA activates GCN2 by displacing the protein kinase moiety from a bipartite tRNA-binding domain. *Mol. Cell* **6,** 269–279 CrossRef Medline
14. Zhang, P., McGrath, B. C., Reinert, J., Olsen, D. S., Lei, L., Gill, S., Wek, S. A., Vattem, K. M., Wek, R. C., Kimball, S. R., Jefferson, L. S., and Cavener, D. R. (2002) The GCN2 eIF2$\alpha$ kinase is required for adaptation to amino acid deprivation in mice. *Mol. Cell Biol.* **22,** 6681–6688 CrossRef Medline
15. Castilho, B. A., Shanmugam, R., Silva, R. C., Ramesh, R., Himme, B. M., and Sattlegger, E. (2014) Keeping the eIF2 $\alpha$ kinase Gcn2 in check. *Biochim. Biophys. Acta* **1843,** 1948–1968 CrossRef Medline
16. Colthurst, D. R., Campbell, D. G., and Proud, C. G. (1987) Structure and regulation of eukaryotic initiation factor eIF-2. Sequence of the site in the $\alpha$ subunit phosphorylated by the haem-controlled repressor and by the double-stranded RNA- activated inhibitor. *Eur. J. Biochem.* **166,** 357–363 CrossRef Medline
17. Pavitt, G. D. (2018) Regulation of translation initiation factor eIF2B at the hub of the integrated stress response. *Wiley Interdiscip. Rev. RNA* **9,** e1491 CrossRef Medline
18. Pakos-Zebrucka, K., Koryga, I., Mnich, K., Ljujic, M., Samali, A., and Gorman, A. M. (2016) The integrated stress response. *EMBO Rep.* **17,** 1374–1395 CrossRef Medline
19. Wek, R. C. (2018) Role of eIF2$\alpha$ kinases in translational control and adaptation to cellular stress. *Cold Spring Harb. Perspect. Biol.* **10,** a032870 CrossRef Medline
20. Wilmes, A., Limonciel, A., Aschauer, L., Moenks, K., Bielow, C., Leonard, M. O., Hamon, J., Carpi, D., Ruzek, S., Handler, A., Schmal, O., Herrgen, K., Bellwon, P., Burek, C., Truisi, G. L., *et al.* (2013) Application of integrated transcriptomic, proteomic and metabolomic profiling for the delineation of mechanisms of drug induced cell stress. *J. Proteomics* **79,** 180–194 CrossRef Medline
21. Ram, B. M., and Ramakrishna, G. (2014) Endoplasmic reticulum vacuolation and unfolded protein response leading to paraptosis like cell death in cyclosporine A treated cancer cervix cells is mediated by cyclophilin B inhibition. *Biochim. Biophys. Acta* **1843,** 2497–2512 CrossRef Medline
22. Ciechomska, I. A., Gabrusiewicz, K., Szczepankiewicz, A. A., and Kaminska, B. (2013) Endoplasmic reticulum stress triggers autophagy in malignant glioma cells undergoing cyclosporine A-induced cell death. *Oncogene* **32,** 1518–1529 CrossRef Medline
23. Chardin, P., and McCormick, F. (1999) Brefeldin A: The advantage of being uncompetitive. *Cell* **97,** 153–155 CrossRef Medline
24. Sano, R., and Reed, J. C. (2013) ER stress-induced cell death mechanisms. *Biochim. Biophys. Acta* **1833,** 3460–3470 CrossRef Medline
25. Sidrauski, C., McGeachy, A. M., Ingolia, N. T., and Walter, P. (2015) The small molecule ISRIB reverses the effects of eIF2$\alpha$ phosphorylation on translation and stress granule assembly. *Elife* **4,** a05033 CrossRef Medline
26. Harding, H. P., Zhang, Y., Zeng, H., Novoa, I., Lu, P. D., Calfon, M., Sadri, N., Yun, C., Popko, B., Paules, R., Stojdl, D. F., Bell, J. C., Hettmann, T., Leiden, J. M., and Ron, D. (2003) An integrated stress response regulates amino acid metabolism and resistance to oxidative stress. *Mol. Cell* **11,** 619–633 CrossRef Medline
27. Ohoka, N., Yoshii, S., Hattori, T., Onozaki, K., and Hayashi, H. (2005) TRB3, a novel ER stress-inducible gene, is induced via ATF4-CHOP pathway and is involved in cell death. *EMBO J.* **24,** 1243–1255 CrossRef Medline
28. Han, J., Back, S. H., Hur, J., Lin, Y. H., Gildersleeve, R., Shan, J., Yuan, C. L., Krokowski, D., Wang, S., Hatzoglou, M., Kilberg, M. S., Sartor, M. A., and Kaufman, R. J. (2013) ER-stress-induced transcriptional regulation increases protein synthesis leading to cell death. *Nat. Cell Biol.* **15,** 481–490 CrossRef Medline
29. Scheuner, D., Song, B., McEwen, E., Liu, C., Laybutt, R., Gillespie, P., Saunders, T., Bonner-Weir, S., and Kaufman, R. J. (2001) Translational control is required for the unfolded protein response and in vivo glucose homeostasis. *Mol. Cell* **7,** 1165–1176 CrossRef Medline
30. Maurin, A. C., Jousse, C., Averous, J., Parry, L., Bruhat, A., Cherasse, Y., Zeng, H., Zhang, Y., Harding, H. P., Ron, D., and Fafournoux, P. (2005) The GCN2 kinase biases feeding behavior to maintain amino acid homeostasis in omnivores. *Cell Metab.* **1,** 273–277 CrossRef Medline
31. Harding, H. P., Zhang, Y., Bertolotti, A., Zeng, H., and Ron, D. (2000) *Perk* is essential for translational regulation and cell survival during the unfolded protein response. *Mol. Cell* **5,** 897–904 CrossRef Medline
32. Lehman, S. L., Ryeom, S., and Koumenis, C. (2015) Signaling through alternative integrated stress response pathways compensates for GCN2 loss in a mouse model of soft tissue sarcoma. *Sci. Rep.* **5,** 11781 CrossRef Medline
33. Schmidt, E. K., Clavarino, G., Ceppi, M., and Pierre, P. (2009) SUnSET, a nonradioactive method to monitor protein synthesis. *Nat. Methods* **6,** 275–277 CrossRef Medline
34. Brazeau, J. F., and Rosse, G. (2014) Triazolo[4,5-d]pyrimidine derivatives as inhibitors of GCN2. *ACS Med. Chem. Lett.* **5,** 282–283 CrossRef Medline
35. Vlahakis, A., Graef, M., Nunnari, J., and Powers, T. (2014) TOR complex 2-Ypk1 signaling is an essential positive regulator of the general amino acid control response and autophagy. *Proc. Natl. Acad. Sci. U. S. A.* **111,** 10586–10591 CrossRef Medline

36. Livi, G. P. (2019) Halcyon days of TOR: Reflections on the multiple independent discovery of the yeast and mammalian TOR proteins. *Gene* **692,** 145–155 CrossRef Medline
37. Burnett, P. E., Barrow, R. K., Cohen, N. A., Snyder, S. H., and Sabatini, D. M. (1998) RAFT1 phosphorylation of the translational regulators p70 S6 kinase and 4E-BP1. *Proc. Natl. Acad. Sci. U. S. A.* **95,** 1432–1437 CrossRef Medline
38. Dennis, P. B., Pullen, N., Kozma, S. C., and Thomas, G. (1996) The principal rapamycin sensitive p70(s6k) phosphorylation sites, T-229 and T-389 are differentially regulated by rapamycin insensitive kinase kinases. *Mol. Cell. Biol.* **16,** 6242–6251 CrossRef Medline
39. Briston, T., Selwood, D. L., Szabadkai, G., and Duchen, M. R. (2019) Mitochondrial permeability transition: A molecular lesion with multiple drug targets. *Trends Pharmacol. Sci.* **40,** 50–70 CrossRef Medline
40. Quirós, P. M., Prado, M. A., Zamboni, N., D'Amico, D., Williams, R. W., Finley, D., Gygi, S. P., and Auwerx, J. (2017) Multi-omics analysis identifies ATF4 as a key regulator of the mitochondrial stress response in mammals. *J. Cell Biol.* **216,** 2027–2045 CrossRef Medline
41. Huang, S., Xing, Y., and Liu, Y. (2019) Emerging roles for the ER stress sensor IRE1α in metabolic regulation and disease. *J. Biol. Chem.* **294,** 18726–18741 CrossRef Medline
42. Yoshida, H., Matsui, T., Yamamoto, A., Okada, T., and Mori, K. (2001) XBP1 mRNA is induced by ATF6 and spliced by IRE1 in response to ER stress to produce a highly active transcription factor. *Cell* **107,** 881–891 CrossRef Medline
43. Kim, J. W., Yang, J. H., Park, H. S., Sun, C., Lee, S. H., Cho, J. H., Yang, C. W., and Yoon, K. H. (2009) Rosiglitazone protects the pancreatic β-cell death induced by cyclosporine A. *Biochem. Biophys. Res. Commun.* **390,** 763–768 CrossRef Medline
44. Hama, T., Nakanishi, K., Mukaiyama, H., Shima, Y., Togawa, H., Sako, M., Nozu, K., Iijima, K., and Yoshikawa, N. (2013) Endoplasmic reticulum stress with low-dose cyclosporine in frequently relapsing nephrotic syndrome. *Pediatr. Nephrol.* **28,** 903–909 CrossRef Medline
45. Lowry, O. H., Rosebrough, N. J., Farr, A. L., and Randall, R. J. (1951) Protein measurement with the Folin phenol reagent. *J. Biol. Chem.* **193,** 265–275 Medline